AD-A112 400 STANFORD UNIV CA EDWARD L GINZTON LAB OF PHYSICS F/G 20/5
RESEARCH STUDIES ON RADIATIVE COLLISIONAL PROCESSES.(U)
JAN 82 S E HARRIS, J F YOUNG F49620-80-C-0023
UNCLASSIFIED GL-3379 AFOSR-TR-82-0121 NL

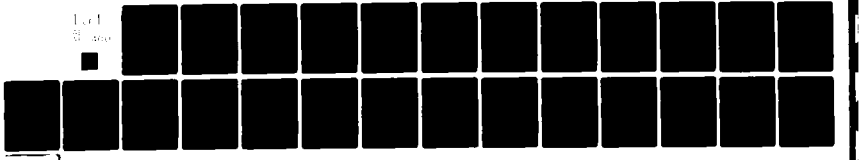

END
DATE FILMED
4-82
DTIC

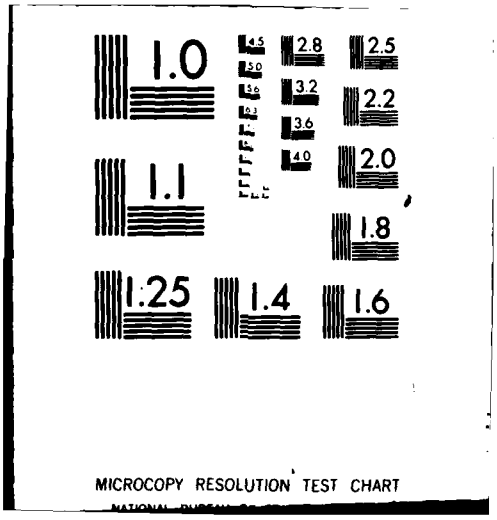
1.0
1.1
1.25
1.4
1.6
1.8
2.0
2.2
2.5
2.8
3.2
3.6
4.0
4.5
5.0
5.6
6.3
MICROCOPY RESOLUTION TEST CHART

(3)

Report F49620-80-C-0023
Annual Technical Report
Project No. 2301/A1

G.L. Report No. 3379

RESEARCH STUDIES ON RADIATIVE COLLISIONAL PROCESSES

S. E. Harris
J. F. Young
Edward L. Ginzton Laboratory
W. W. Hansen Laboratories of Physics
Stanford University
Stanford, California 94305

January 1982

Annual Technical Report for Period 1 October 1980 – 30 September 1981

Contract Monitor:

Dr. Howard R. Schlossberg
AFOSR/NP
Bolling Air Force Base
Building 410
Washington, D.C. 20332

UNCLASSIFIED

SECURITY CLASSIFICATION OF THIS PAGE (When Data Entered)

REPORT DOCUMENTATION PAGE	READ INSTRUCTIONS BEFORE COMPLETING FORM
1. REPORT NUMBER AFOSR-TR- 82-0121 2. GOVT ACCESSION NO. AD-A115470	3. RECIPIENT'S CATALOG NUMBER
4. TITLE (and Subtitle) RESEARCH STUDIES ON RADIATIVE COLLISIONAL PROCESSES	5. TYPE OF REPORT & PERIOD COVERED Annual Technical Report 1 Oct. 80 – 30 Sept. 81
	6. PERFORMING ORG. REPORT NUMBER G.L. Report No. 3379
7. AUTHOR(s) S. E. Harris J. F. Young	8. CONTRACT OR GRANT NUMBER(s) F49620-80-C-0023
9. PERFORMING ORGANIZATION NAME AND ADDRESS Edward L. Ginzton Laboratory Stanford University Stanford, CA 94305	10. PROGRAM ELEMENT, PROJECT, TASK AREA & WORK UNIT NUMBERS 61102F 2301/A1
11. CONTROLLING OFFICE NAME AND ADDRESS Air Force Office of Scientific Research Building 410 Bolling AFB, DC 20332	12. REPORT DATE January 1982
	13. NUMBER OF PAGES 24
14. MONITORING AGENCY NAME & ADDRESS(if different from Controlling Office)	15. SECURITY CLASS. (of this report) UNCLASSIFIED
	15a. DECLASSIFICATION/DOWNGRADING SCHEDULE

16. DISTRIBUTION STATEMENT (of this Report)

Approved for public release; distribution unlimited

17. DISTRIBUTION STATEMENT (of the abstract entered in Block 20, if different from Report)

18. SUPPLEMENTARY NOTES

19. KEY WORDS (Continue on reverse side if necessary and identify by block number)

Laser Induced Collisions
VUV Spectroscopy
Excimer Lasers

20. ABSTRACT (Continue on reverse side if necessary and identify by block number)

This program has supported theoretical and experimental studies in three broad areas. The first is a study of pair absorption processes which may be viewed as a collisional process in which two atoms and a photon simultaneously react and exchange energy. The present goal is to investigate the possibility of using such processes to construct new types of lasers. Secondly, we have invented and developed a promising new technique for pumping high pressure gas systems using high power microwave pulses. This work has led to two

DD FORM 1 JAN 73 1473 EDITION OF 1 NOV 65 IS OBSOLETE S/N 0102 LF 014-6601

UNCLASSIFIED

SECURITY CLASSIFICATION OF THIS PAGE (When Data Entered)

1. INTRODUCTION

This program has supported theoretical and experimental studies in three broad areas. The first is a study of pair absorption processes which may be viewed as a collisional process in which two atoms and a photon simultaneously react and exchange energy. The present goal is to investigate the possibility of using such processes to construct new types of lasers. Secondly, we have invented and developed a promising new technique for pumping high pressure gas systems using high power microwave pulses. This work has led to two related projects: excitation of rare gas halide excimer lasers to achieve long pulse lengths, high reliability and good efficiencies, and the excitation of metal vapors to create new lasers. Finally, we have been applying the anti-Stokes light source developed here to practical measurements of VUV spectral features both to elucidate the physics of such innershell transitions and to search for transitions suitable for short wavelength lasers. This last project has also been partially supported by NASA.

Section 2 summarizes our research findings for these projects, and Sections 3 and 4 list the publications and personnel, respectively, supported by this program. Our previous work under this contract on laser induced charge exchange has been concluded and the results [illegible]hed. A reprint is included as Appendix A.

2. SUMMARY OF RESEARCH

A. Pair Absorption Processes

Pair absorption refers to a process in which two colliding atoms simultaneously absorb a single photon at a frequency corresponding to the sum energy of the two product species. The process may be viewed as an excitation to a virtual level followed by collision, or alternately as an absorption by a quasi-molecule formed during collision. Pair absorption provides a general method for optically pumping the upper levels of both allowed and non-allowed transitions.

In particular, Falcone has noted that pair absorption pumping allows the inversion of the less dense of the two species with regard to its ground level. For a nondegenerate system, with excited state densities N_A^* and N_B^*, and ground state densities N_{AG} and N_{BG}, the equilibrium of the pair absorption process is $N_A^* N_B^* = N_{AG} N_{BG}$. For N_{BG} greater than N_B^*, N_A^* is greater than N_{AG}, and species A is inverted. The method may be used to invert non-allowed, as well as allowed transitions.

The first example of lasing by pair absorption pumping was demonstrated by Falcone and Zdasiuk.[1] The system, employing Ba and Tl, was pumped at 3867 Å and produced lasing at 1.5 μm. As a continuation of this work we proposed to attempt an inversion to ground via pair absorption pumping in Ba-Sr; however, the high pump power ($\sim 2.25/cm^2$) required created severe difficulties, one of which was photoionization of the final states. It was clear that a

[1] R. W. Falcone and G. A. Zdasiuk, Opt. Lett. 5, 155 (1980).

better system would be more viable for the proposed study. A system that contained one species with a split ground state (such as Tl or In) would be a good candidate as the threshold requirements would be relaxed in that the lower laser level would be considerably less populated than the ground state. Furthermore, if the pair absorption coincided with a known excimer the pair absorption could provide a means of converting the excimer into the visible.

At the close of the last reporting period we were beginning an extensive search for possible excimer pumped pair absorption systems that would lase in the visible. Over thirty-four elements were included in a computerized search for pair absorptions that would coincide with a known excimer or efficient ultraviolet laser. The results yielded twenty-six possible pair processes (Table 1); however, only four of these coincide with existing excimers. Of these four only one, Ba-Na, has a strong absorption coefficient, and even this scheme would require inversion to ground to obtain a laser. It is clear that useful coincidences are rare.

The results of the search are not totally discouraging, as it points out the possibility of studying in detail pair absorption lasers. The second entry in Table 1, Pb-In, has a strong absorption coefficient and it has an output laser wavelength in the visible (Fig. 1). Lasing in this system will occur on the 4511 Å line of indium to its split ground state. The advantage of this scheme is that it will be easier to invert to the $5p\ ^2P^o_{3/2}$ than to the $5p\ ^2P^o_{1/2}$ because initially the $^2P^o_{3/2}$ will have a lower population. Furthermore, the gain on this line is slightly higher. The absorption coefficient for this system has been measured recently and found to be 4.7×10^{-36} [In][Pb], which is larger than the calculated value of 1.8×10^{-36} [In][Pb]. Combined with an indium density of $\sim 10^{16}$ cm^{-3} this yields a modest pump energy density of 0.2 J/cm^2

Table 1

Ultraviolet Pair Absorptions [a]

Elements	Pump Laser (Å)	Output Laser (Å)	Absorption Coefficient [b]
Pb-Gd	2828 (XeBr) [c]	5576	7.3×10^{-37}
Pb-In	2855	4511	1.8×10^{-36}
Tℓ-Ba	2751	5826	5.3×10^{-37}
Pb-Ba	2749	5826	5.0×10^{-38}
Pb-Tℓ	2693	5352	6.0×10^{-38}
Sn-Sc	2478 (KrF)	5020	8.6×10^{-38}
In-Pb	2667	4059	5.8×10^{-38}
In-Gd	3933	5938	1.2×10^{-37}
Ba-Gd	2945	6336	1.4×10^{-37}
Pb-Gd	2832	6926	7.4×10^{-35}
Pb-Gd	2953	5938	6.4×10^{-38}
Tℓ-Na [d]	4038	--	2.6×10^{-37}
Tℓ-Eu	3384	--	1.7×10^{-37}
In-Ca	3866	--	3.4×10^{-37}
In-Eu [d]	4171	--	2.1×10^{-36}
In-Tm	3765	--	6.3×10^{-38}
Ba-Li	3803	--	3.1×10^{-37}
Ba-Na	3527 (XeF)	--	2.0×10^{-35}
Ba-Ca	2853	--	2.0×10^{-37}
Ba-Eu	3016	--	1.7×10^{-36}
Pb-Ca	2915	--	5.5×10^{-37}
Pb-Eu	3085 (XeCℓ)	--	7.8×10^{-38}
Pb-Tm	2857	--	1.4×10^{-36}
Pb-Tm	2852	--	6.5×10^{-37}
Pb-Tm	2664	--	2.4×10^{-38}
Pb-Yb	2800	--	2.2×10^{-36}

[a] This table is not exhaustive nor does it include the Ba-Sr, Ba-Tℓ, or Ba-Ba systems that have already been observed.

[b] The absorption coefficient shown should be multiplied by the product of the ground state number densities (in cm^{-3}) to obtain the fractional absorption per centimeter.

[c] If the pump laser should lie within 10 Å of a known excimer laser the corresponding excimer is listed following the pump wavelength.

[d] These systems were included as they may be useful for inversion to ground even though the pump is greater than 4000 Å.

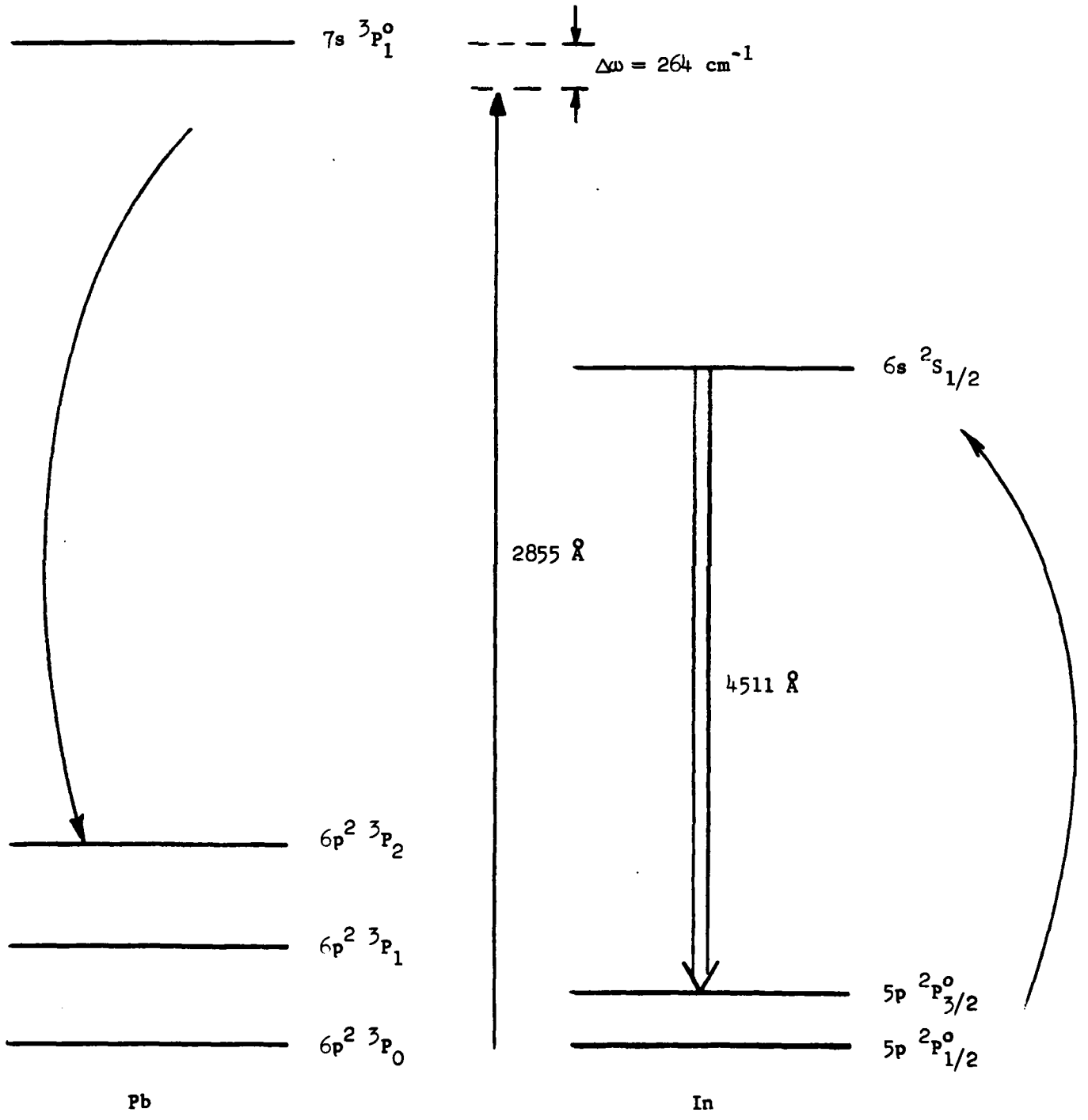

Fig. 1--Energy level diagram of pair absorption laser.

(compared to 2.2 J/cm^2 for Ba-Sr). Finally, the problem of Raman gain into the lower laser level is minimized as the threshold for this process requires a $\Delta N = 5 \times 10^{17}\ cm^{-3}$, which is a factor of 50 larger than current operating parameters.

In summary, the Pb-In system should provide a means of studying such effects as defocusing of the pump beam (i.e., beam blow-up) when pumping pair absorptions with high powers, the interplay of Raman and pair absorption processes, the polarization of the output laser with respect to the pump, and, finally, it would bring us closer to the realization of using pair absorption to invert a species to its ground state.

B. Microwave Pumped Excimer Lasers

During the past year, we have concentrated on improving the operation of the microwave pumped $XeCl^*$ laser. The goal has been to improve the 0.006% efficiency previously reported and to extend the pulse length beyond the earlier 100 ns limit. Higher efficiencies and longer pulse lengths could make the microwave pumped $XeCl^*$ laser a viable source of good mode quality, short UV pulses by the use of traditional mode locking techniques which are not generally possible with dc discharge excimer lasers due to the short pulse lengths. Microwave excitation should also result in improved lifetime and reliability.

As previously reported, a 600 kW magnetron was used to pump the gas mixture in a 3 mm diameter quartz tube. Using this power source, 150 ns pulses with peak powers of ~ 500 W have been attained representing an efficiency of ~ 0.1%. This is in contrast to the 100 ns pulses with peak powers of ~ 30 W reported earlier. Repetition rates have also been improved from 10 Hz to over 400 Hz but with significantly reduced performance at the high repetition rates.

Using a new Varian SFD-303B coaxial magnetron which can provide up to 1.4 MW, 3.5 μs long pulses at 9.375 GHz, pulse lengths of 200 ns have been observed but at reduced peak powers of ~ 250 W representing an efficiency of ~ 0.03%. The laser cell used with the new Varian magnetron differed slightly from that previously reported in that an exchangeable coupling plate was employed to allow for optimizing the microwave power deposition into the gain medium. Also, preionization by the low pressure xenon tube was no longer used. The best coupling observed with this design was 100% absorption for the first 500 ns of the pump pulse followed by a decrease to 50% rf absorption. The laser action occurred at the point of maximum fluorescence which coincided with the drop in rf absorption. Repetition rate in this design was limited to 190 Hz.

The 200 ns pulses obtained with the 1.4 MW magnetron had a lower efficiency than the 150 ns pulses obtained with the 600 kW source largely because of the difference of the input power. Presently we are redesigning the laser cell with a smaller tube radius and a confocal resonator to achieve higher power deposition per unit volume. This new design will have a smaller active volume and thus allow a smaller pump source to achieve the equivalent or higher power density in the gain medium as the 1.4 MW source with the previous design. This should improve efficiencies provided the microwave power can be absorbed in the smaller volumes.

The absorption in the present cell is presumably limited by a high electron density screening out the microwaves after the first 500 ns resulting in the observed 50% decrease in rf absorption. A finite skin depth is evident by a ~ 1 mm ring of bright visible fluorescence at the edge of the plasma. For a uniform plasma, the absorption skin depth is proportional to $(\nu_c/\omega n_e)^{1/2}$,

where ν_c is the collision frequency, n_e is the electron density, and ω is the microwave frequency; our qualitative observations indicate that as the pressure is increased n_e increases faster than ν_c resulting in shorter skin depths and nonuniform excitation. The new design with the decreased tube radius will thus not only increase the power deposition per unit volume but also alleviate the skin depth problem.

In addition, a new gas manifold is also under construction to accompany the new laser design. In response to previous contamination problems, the new recirculating system is constructed largely of nickel, which is particularly corrosion resistant to HCℓ gas. Furthermore, a filter and a molecular sieve have been added to prevent contamination by ferrous chloride particles released by the HCℓ tank and to prevent pump oil vapor from entering the recirculating system. To help characterize and improve the conditions for high repetition rates, provisions have been made to cool the gas and monitor its mass flow rate.

In general, the new manifold and laser design will reduce contamination of the laser mixture while increasing the power per unit volume deposited in the active region. This method of increasing the power density by decreasing the active volume offers the possibility of higher efficiencies in the microwave pumped XeCℓ* laser and of pumping lower gain excimer systems.

C. Development of a Tunable Narrowband XUV Light Source

Based on the proposal of Harris,[1] we have developed a new light source in the extreme ultraviolet. The source is based upon the scattering of a tunable visible laser off excited helium metastable atoms (spontaneous

[1] S. E. Harris, Appl. Phys. Lett. 31, 498 (1977).

anti-Stokes Raman scattering). Photons of energy equal to the sum of the helium storage energy and the incident laser photon energy are time gated with the incident laser and have a very narrow bandwidth (the convolution of the laser bandwidth and the Doppler width of the helium atoms).

In the first experiment[1] we measured the absorption spectra of potassium in the spectral interval 535.4 Å – 546.5 Å (182,975 cm^{-1} – 186,679 cm^{-1}) with a resolution of approximately 1.3 cm^{-1}. The experimental apparatus used and recorded absorption scans of potassium are shown in Figs. 2 and 3. Note that the apparatus involves no spectrometer. This is possible because the discharge is being operated at very low current so that the background radiation from the discharge is at a minimum. The anti-Stokes light is then seen on top of this constant background.

The extent of tunability in this first experiment was limited by the brightness of the source. Since then we have embarked on a new apparatus design which has greatly increased brightness, signal to noise, and hence tuning range. The present appratus design is shown in Fig. 4. Here we have introduced an intense pulsed discharge to the system. One result of this is an expected increase in helium metastable population (and hence anti-Stokes brightness) by roughly a factor of 100. Another result of the introduction of this pulsed discharge is a much greater increase in the background from the discharge. Hence, we have found it necessary to insert a spectrometer into the system which serves as a rejection filter against the intense background radiation while passing the anti-Stokes light. The result of these modifications is that we have increased the signal to noise of the anti-Stokes light by a factor of roughly 20 over the first experiment.

---

[1] J. E. Rothenberg, J. F. Young, and S. E. Harris, Opt. Lett. 6, 363 (1981).

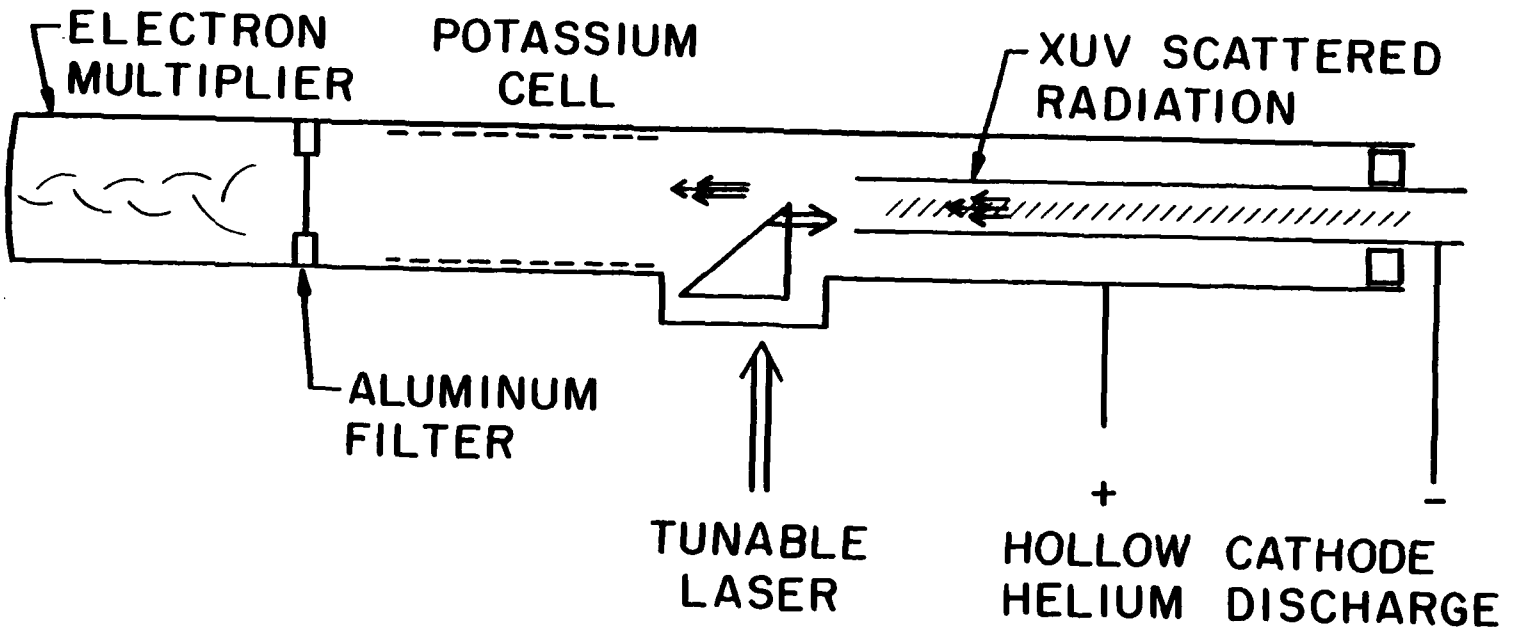

Fig. 2--Schematic of apparatus used for absorption spectroscopy of potassium.

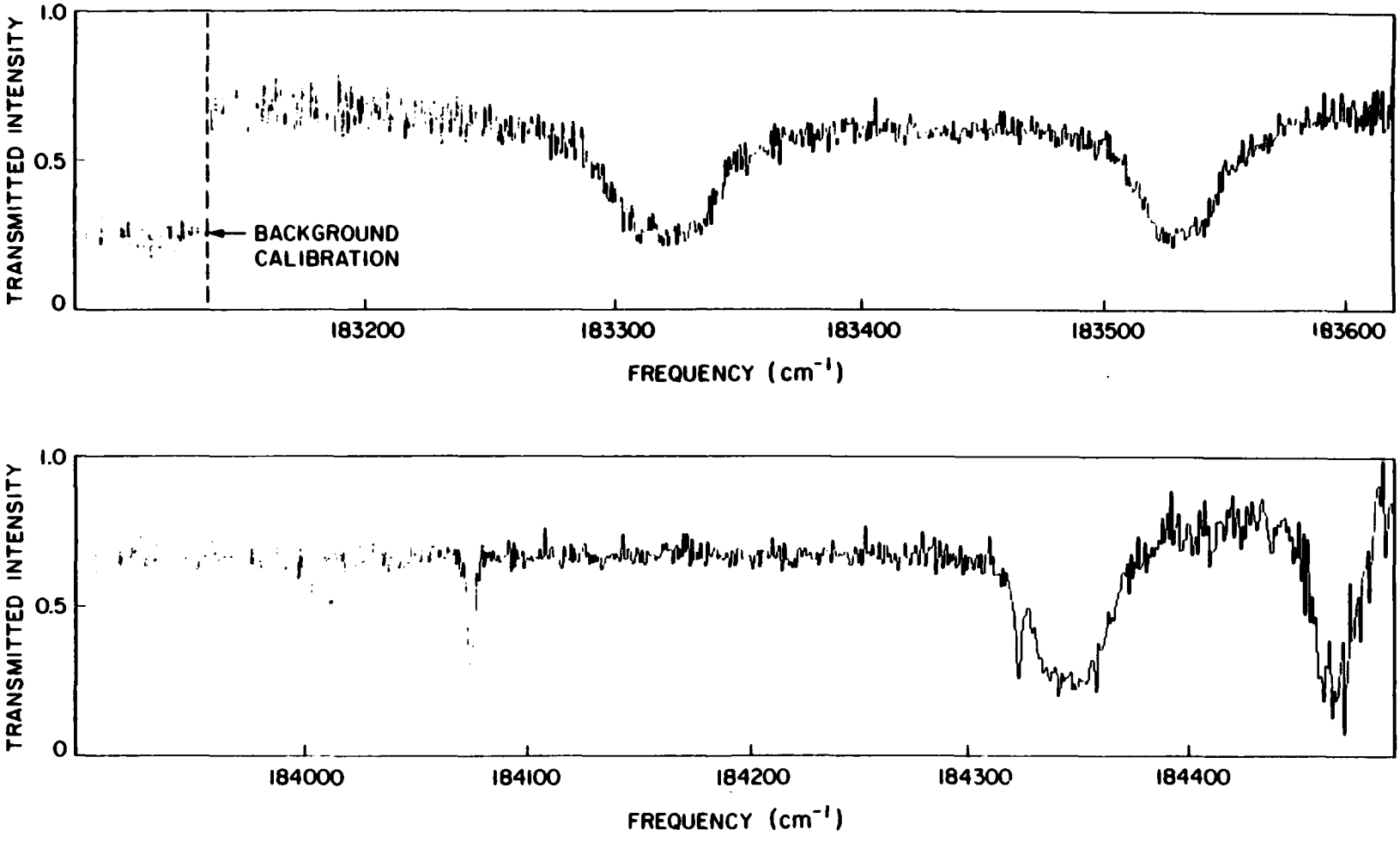

Fig. 3--Absorption scans of potassium. Vapor pressure is 10^{15} atoms/cm^3, and cell length is 5 cm.

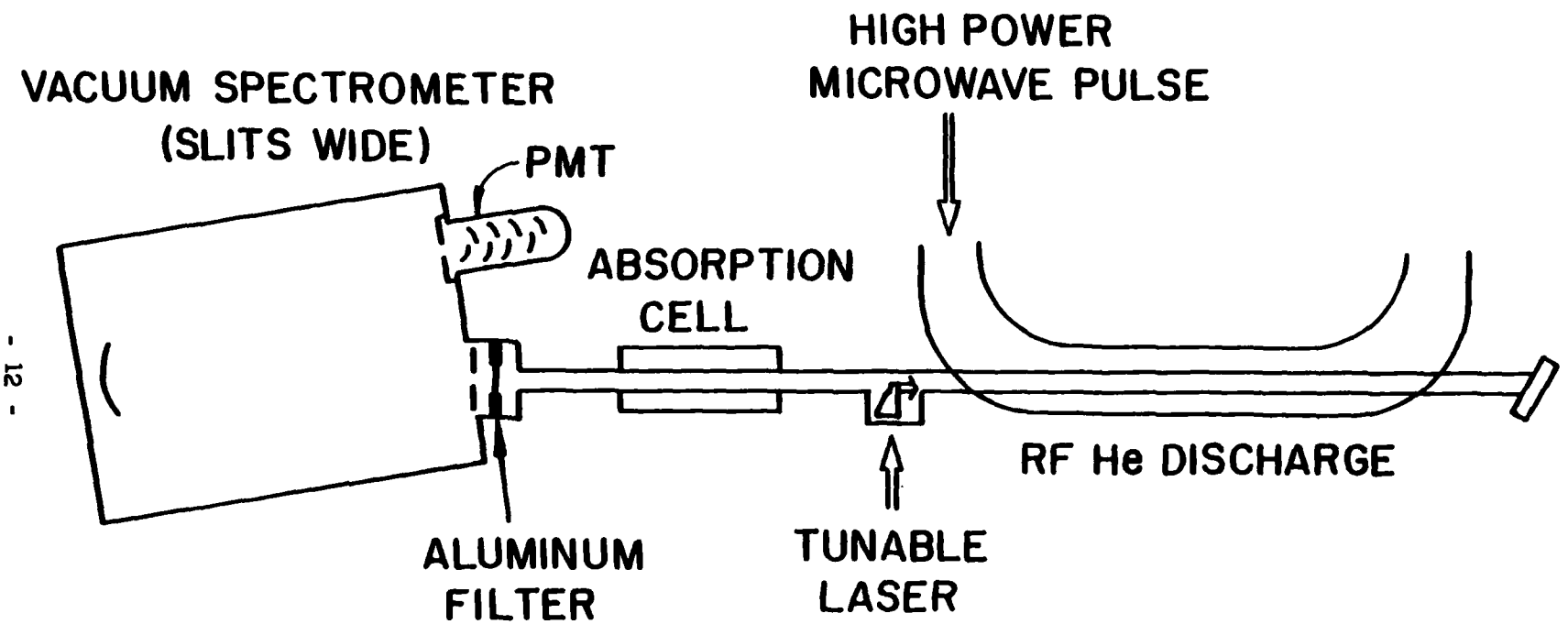

Fig. 4--Apparatus for absorption spectroscopy using microwave pumped anti-Stokes light source.

With the increased tunability we expect, we intend to first examine a more complete spectral range in the innershell excitation of potassium. The source then may be used for examination of Rydberg autoionizing states and other states interesting for possible laser construction in the 500 Å region. In addition, the source can be used in conjunction with an electron detection apparatus to examine excitation of autoionizing states by detecting the subsequently ejected electrons after exciting the states with the anti-Stokes light source.

D. Microwave Pumping of Metal Vapors

We are currently investigating the possibility of obtaining large populations of metal vapor atoms in excited electronic states by using microwave pumping. Intense microwave fields are used to ionize metal atoms, which subsequently recombine with electrons through a process of three-body recombination. Recombination occurs preferentially into higher energy levels, thereby creating large excited state populations. Particularly interesting are the long-lived states because large amounts of energy can be stored in them. This stored energy can then be used for various collisional and radiative transfer processes. The use of microwaves as a pump is attractive for several reasons. Electromagnetic fields in the GHz range couple power into a plasma much more effectively than radio frequency or dc fields. That means that microwave discharges can be more efficient, and sustained for longer periods of time. Also, the relative maturity of that particular technology makes high power microwave sources commercially available. A microwave pumped excimer laser built in our group[1] has already demonstrated a number of advantages of microwave pumping.

[1] A. J. Mendelsohn, R. Normandin, S. E. Harris, and J. F. Young, Appl. Phys. Lett. 38, 603 (April 1981).

Over the past year, a system has been set up for microwave pumping of metal vapors, and has been used to study the excitation of Sr. vapor. The objective is to populate the 5s5p $^3P^o$ level of Sr, which is a weakly allowed transition to ground at 6893 Å. It has been shown[1] that the level in question is efficiently populated, by collisional and radiative processes, from other states. If this state inverts with respect to ground, it could be Q-switched to obtain high peak power pulses. Even if no inversion occurs, the long lifetime (~ 75 μs) of this state offers attractive energy storage. The apparatus consists of a metal vapor cell that has been specially designed so that the microwave power can be coupled into the cell. Metal vapor is contained in a dielectric tube, which rests on the bottom of a stainless steel tube. The steel tube contains two compartments that serve as waveguides and there are coupling slots between them. Power from a 60 kW peak power magnetron is delivered to one waveguide, and is coupled uniformly with distance to the waveguide that contains the dielectric tube. In this way, plasma is generated in the dielectric tube, and Sr atoms become electronically excited through plasma recombination. The whole cell is heated from the outside to maintain a desired vapor pressure of Sr.

In the first round of this experiment, we were unable to obtain a large population in the Sr 5s5p $^3P_1$ state. This may have been due to the coating of the alumina tube by the Sr atoms, thereby partially shielding out the microwave field. We have recently purchased some sapphire tubes, and preliminary results look qualitatively encouraging, in that the discharge is much brighter, and it is now bluish, characteristic of the Sr resonance line radiation.

---

[1] J. J. Wright and L. C. Balling, J. Chem. Phys. 73, 1617 (August 1980); P. P. Sorokin and J. R. Lankard, Phys. Rev. 186, 186 (October 1969).

In the next few weeks, we expect to use the transient absorption of a probe laser beam to measure the excited state population. If we succeed in obtaining a large population, we plan to use it to demonstrate a radiative collision laser for the first time.

3. PUBLICATIONS

1. R. W. Falcone and G. A. Zdasiuk, "Pair Absorptin Pumped Barium Laser," Optics Lett. 5, 155 (April 1980).
2. R. W. Falcone and G. A. Zdasiuk, "Radiative Collisional Fluorescence Observed From Thermally Excited Atoms," Optics Lett. 5, 365 (September 1980).
3. S. E. Harris, J. F. Young, R. W. Falcone, W. R. Green, D. B. Lidow, J. Lukasik, J. C. White, M. D. Wright, and G. A. Zdasiuk, "Laser Induced Collisional Energy Transfer," in Atomic Physics VII, D. Klepner and F. M. Pipkin, eds. (New York: Plenum Press, 1981).
4. A. J. Mendelsohn, R. Normandin, S. E. Harris, and J. F. Young, "A Microwave Pumped $XeCl^*$ Laser," Appl. Phys. Lett. 38, 603 (April 1981).
5. Joshua E. Rothenberg, J. F. Young, and S. E. Harris, "High Resolution XUV Spectroscopy of Potassium Using Anti-Stokes Radiation," Optics Lett. 6, 363 (August 1981).
6. M. D. Wright, D. M. O'Brien, J. F. Young, and S. E. Harris, "Laser Induced Charge Transfer Collisions of Calcium Ions With Strontium Atoms," Phys. Rev. A 24, 1750 (October 1981).
7. S. E. Harris, R. W. Falcone, M. Gross, R. Normandin, K. D. Pedrotti, J. E. Rothenberg, J. C. Wang, J. R. Willison, and J. F. Young, "Anti-Stokes Scattering as an XUV Radiation Source," in Laser Spectroscopy V, A. R. W. McKellar, T. Oka, and B. P. Stoicheff, eds. (New York: Springer-Verlag, 1981).

4. PERSONNEL

R. W. Falcone

S. E. Harris

A. J. Mendelsohn

R. J. F. Normandin

D. M. O'Brien

B. Petek

J. E. Rothenberg

P. J. K. Wisoff

J. F. Young

APPENDIX A

Laser-induced charge-transfer collisions of calcium ions with strontium atoms

M. D. Wright, D. M. O'Brien, J. F. Young, and S. E. Harris
Edward L. Ginzton Laboratory, Stanford University, Stanford, California 94305
(Received 23 April 1981)

Experimental studies of two laser-induced charge-transfer reactions in Ca and Sr are presented. In both reactions, a Ca ion collides with an Sr neutral in the presence of a laser field to produce a Ca neutral and an excited Sr ion. The two reactions differ in the final level of the Sr^+ species. The collision cross sections associated with these reactions are studied as functions of applied laser frequency and power density. The largest cross section induced is equal to 10^{-16} cm^2, obtained at a power density of 2×10^9 W/cm^2. Differences in experimental results associated with the two reactions are explained qualitatively by an examination of the potential curves of the $CaSr^+$ quasimolecule.

I. INTRODUCTION

Laser-induced collision processes constitute a technique for energy transfer in atomic systems and as such may have application to the development of high-energy visible and ultraviolet lasers. For example, an electrical discharge might be used to create a large metastable population in one species and the stored energy could then be rapidly transferred by laser-induced collisions to a lasing level in a second species. A laser-induced charge-transfer collision[1-5] is a particularly interesting process in that it exploits a high-capacity storage species, ground-state ions. Ions are easily created and have long lifetimes.

In this publication we present an experimental study of two laser-induced charge-transfer collision processes:

$$Ca^+(4s\,^2S_{1/2})+Sr(5s^2\,^1S_0)+\hbar\omega(4715\ \text{Å})\rightarrow Ca(4s^2\,^1S_0)+Sr^+(5p\,^2P^o_{3/2}), \quad (1a)$$

$$Ca^+(4s\,^2S_{1/2})+Sr(5s^2\,^1S_0)+\hbar\omega(4795\ \text{Å})\rightarrow Ca(4s^2\,^1S_0)+Sr^+(5p\,^2P^o_{1/2}). \quad (1b)$$

An energy-level diagram pertinent to both processes is shown in Fig. 1. Without the laser photon the processes of Eq. (1) are endothermic and have a vanishingly small collision cross section. The laser photon supplies necessary energy and may be thought of as raising one of the two Sr valence electrons to a virtual level of $Sr(5s\,5p\,^1P^o_1)$ character. The Sr atom in a virtual level then collides with a ground-state Ca ion which captures the remaining Sr valence electron, leaving a Ca ground-state neutral and an excited Sr ion.

The laser-induced charge-transfer collisions given by Eqs. (1a) and (1b) appear quite similar, the final levels of the target species differing only in J value. However, there are significant differences in the character of the two reactions. In a laser-induced charge-transfer collision, the collision cross section maximizes at a wavelength which is detuned from the wavelength of the photon which exactly satis-

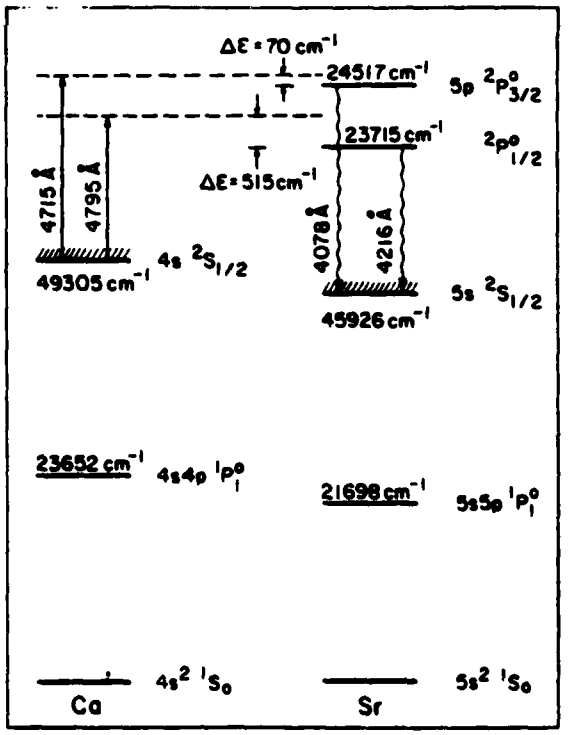

FIG. 1. Energy level diagram for laser-induced charge-transfer reactions (1a) and (1b).

fies the energy defect between the initial and final states of the collision system when the colliding species are infinitely separated ($\lambda_{R=\infty}$). As indicated in Fig. 1, the cross section associated with reaction (1a) maximizes when the photon is 70 cm^{-1} more energetic than $\lambda_{R=\infty}$, while the cross section associated with reaction (1b) maximizes when the photon is 515 cm^{-1} more energetic than $\lambda_{R=\infty}$. Also, the values and line shapes of the cross sections for reactions (1a) and (1b) are considerably different. These differences are a result of the quasimolecular potentials associated with the different target levels.

II. APPARATUS

In order to observe the charge-transfer processes described by Eqs. (1a) and (1b), two lasers are used: one to produce Ca^+ population for energy storage, and the second to affect energy transfer to the excited Sr^+ level. A schematic of the optical system employed to observe reaction (1a) is shown in Fig. 2. An actively mode-locked and Q-switched Nd:YAG (yttrium aluminum garnet) oscillator generates ~2 mJ of 1.06-μm radiation in a train of pulses. Each pulse is 100 ps in duration and there are about 10 pulses in the train. The pulse train is amplified by a series of Nd:YAG amplifiers having a final aperture of 0.95 cm and typically supplying a total of 300 mJ. Two KD*P (potassium dideuterium phosphate) crystals are used to generate 3547-Å radiation by successive second harmonic generation and mixing. The ~90 mJ of 3547-Å radiation is separated by a prism, split, and used to pump two dye lasers. Each dye laser is synchronously pumped,[6] prism tuned, and cavity dumped to produce a single 40 ps pulse of tunable visible radiation with an energy of from 0.1 to 0.5 mJ and a linewidth of ~10 cm^{-1}. The two dye laser pulses are spatially combined with a dichroic mirror and focused to an area of 10^{-3} cm^2 inside the metal vapor cell. Thus, power densities of several GW/cm^2 are available. The metal vapor cell is heated to ~850°C and produces ground-state densities of about 10^{16} cm^{-3} of both Sr and Ca; 15 torr of argon buffer gas is used to protect the cell windows.

The wavelength of the pump dye laser is tuned to 5361 Å, which corresponds to the $Ca(4s^2\,{}^1S_0)$-$Ca(4s\,4d\,{}^1D_2)$ two-photon transition. Ca ions are produced by resonantly enhanced three-photon ionization. The pulse from the transfer laser arrives in the cell 5 ns after the pump laser pulse to eliminate possible two-photon effects. Back-directed fluorescence from the target level population created by the laser-induced charge-transfer process is collected by a mirror with a hole in it and focused into a 1-m spectrometer having a resolution of 2.5 Å and an RCA 31034 photomultiplier at its exit slit.

In order to observe the laser-induced charge-transfer process denoted by Eq. (1b), more energy in the transfer laser pulse is required than that which can be delivered by the transfer laser system described above. Therefore, a Quanta-Ray PDL dye laser is used as the transfer laser. A schematic is shown in Fig. 3. The Quanta-Ray dye laser produces about 10 mJ in the desired wavelength region with a spectral linewidth of about 0.5 cm^{-1} and a pulse duration of 5 ns. In this configuration the transfer laser pulse follows the pump laser pulse by about 30 ns. The longer delay between pump and transfer laser pulses is necessary because of the greater jitter in pulse timing using two independent lasers.

In both charge-transfer experiments the transfer laser wavelength is scanned and the intensity of fluorescence from the target level population is

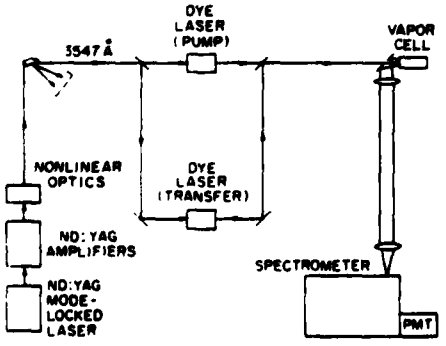

FIG. 2. Schematic of optical system used to observe reaction (1a).

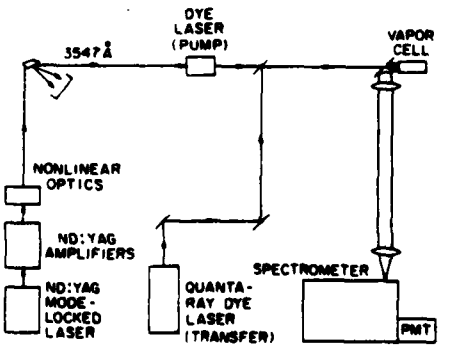

FIG. 3. Schematic of optical system used to observe reaction (1b).

recorded both as a function of the transfer laser wavelength and as a function of time. Time resolution is accomplished by processing the signal from the photomultiplier with four electronic integrators which are gated on during consecutive 10-ns time intervals. The outputs of the integrators are input to a Cromemco *Z-2D* minicomputer which stores the information on a disk for later data smoothing.

Determination of collision cross sections associated with reactions (1a) and (1b) requires the measurement of the initial Ca^+ population density as well as the measurement of the excited Sr^+ densities. Excited Sr^+ densities are determined from the fluorescent signals which are produced during the experimental procedures described above. The Ca^+ population density is determined by measuring the absorption of a probe beam at 3934 Å corresponding to the $Ca^+(4s\ ^2S_{1/2})$-$Ca^+(4p\ ^2P^o_{3/2})$ transition. The apparatus used to make this measurement is the same as that shown in Fig. 3, with the modification that the spectrometer is moved directly behind the cell such that the probe laser beam passes through the entrance slit of the spectrometer after emerging from the cell.

III. RESULTS

Scans associated with reaction (1a) are presented in Fig. 4. In this figure, fluorescence at 4078 Å is plotted as a function of transfer laser wavelength for each of the sequential 10-ns observation time intervals. The laser-induced charge-transfer signal peaks at 4715 Å. The line shape associated with this process is characterized by a slight tail on the blue side of the peak and a width of $\sim 50\ cm^{-1}$ full width at half maximum (FWHM). The other peaks in these scans represent noise processes and correspond to known single- or two-photon transitions in Sr or Ca. When the transfer laser is tuned to 4607 Å, for example, $Sr(5s\,5p\ ^1P^o_1)$ atoms are produced; these excited atoms collide with ground-state Ca^+ to produce $Sr^+(5p\ ^2P^o_{3/2})$ population by way of normal exothermic ($\sim 600\ cm^{-1}$) charge transfer.[7] The importance of time resolved detection is now apparent in that the laser-induced charge-transfer signal decays rapidly relative to the other lines. In the laser-induced collision process, energy transfer occurs only when the laser field is present; hence, fluorescence from the target state must maximize during the time the transfer laser pulse is present and then decay at a rate which is commensurate with the lifetime of the target state,

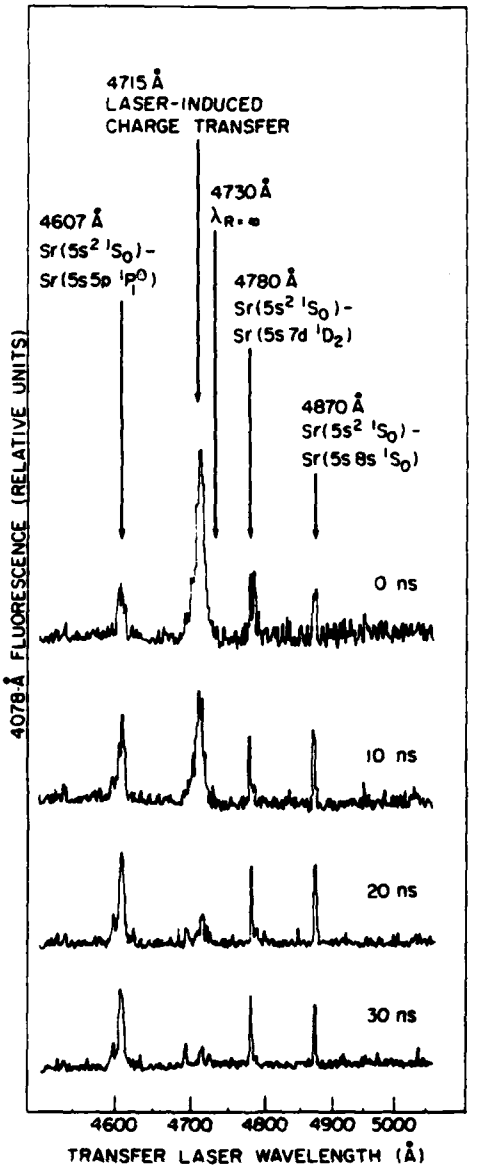

FIG. 4. Fluorescence from $Sr^+(5p\ ^2P^o_{3/2})$ population as a function of transfer laser wavelength and time.

which in this case is approximately 7 ns.[8] In the other processes, energy transfer occurs as long as ions and excited neutrals are present; since these species exist for long times, so also does fluorescence.

Figure 5 presents scans associated with reaction (1b). Fluorescence at 4216 Å is plotted as a function of transfer laser wavelength for the different observation time intervals. The laser-induced charge-transfer signal is the broad curve peaking at 4795 Å and upon which other narrow lines are superimposed. The linewidth of this process is ~ 300

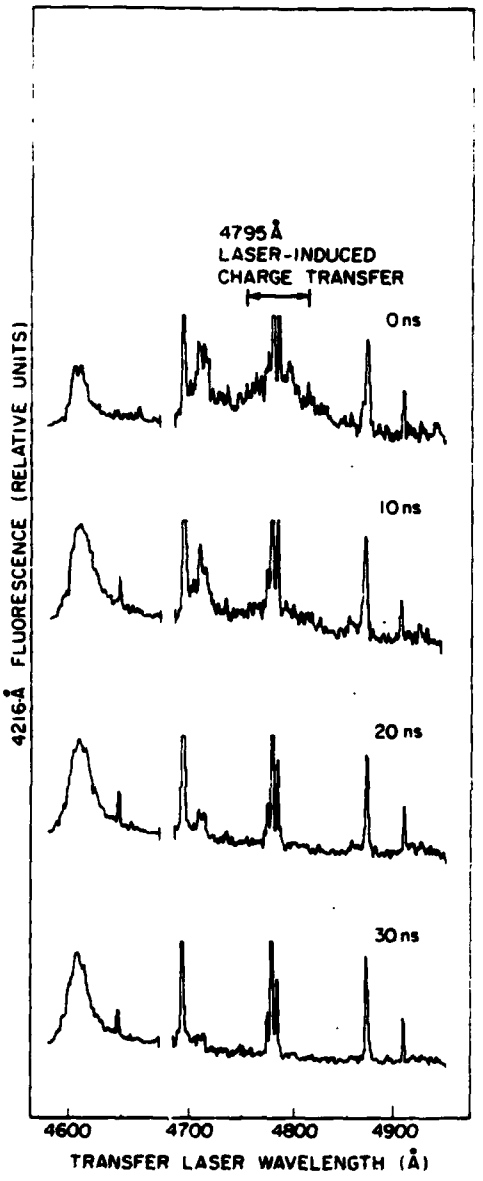

FIG. 5. Fluorescence from $Sr^+(5p\ ^2P^o_{1/2})$ population as a function of transfer laser wavelength and time. Signals at 4607, 4648, 4694, 4775, 4780, 4785, 4870, and 4910 Å correspond to single- and two-photon transitions in Sr and Ca, and are not labeled for purposes of clarity. The vertical sensitivity is increased by a factor of 13 at 4685 Å.

cm^{-1}, and the shape is roughly symmetrical. Note again the rapid decay of the laser-induced charge-transfer signal relative to the other lines. One exception is the line at 4715 Å, which also decays rapidly with time. The kinetics associated with this peak are probably as follows: Radiation at 4715 Å populates the $Sr^+(5p\ ^2P^o_{1/2})$ level via laser-induced charge-transfer collisions; inelastic collisions then transfer this excitation to the $Sr^+(5p\ ^3P^o_{1/2})$ level, which fluoresces at 4216 Å. Since the $Sr^+(5p\ ^2P^o_{3/2})$ population decays rapidly, so must the $Sr^+(5p\ ^3P^o_{1/2})$ population.

Several diagnostic measurements were made to confirm the interpretation of the peaks at 4715 and 4795 Å as due to laser-induced charge-transfer collisions. These were: (1) detuning the pump laser by 10 Å from the $Ca(4s^2\ ^1S_0)$-$Ca(4s\,4d\ ^1D_2)$ two-photon transition eliminated the $Ca^+(4s\ ^2S_{1/2})$ population and caused the signals at 4715 and 4795 Å to disappear; the two-photon noise lines remained; (2) tuning the pump laser to the $Sr(5s^2\ ^1S_0)$-$Sr(5p^2\ ^1S_0)$ two-photon transition produced $Sr^+(5s\ ^2S_{1/2})$ population; no signals at 4715 or 4795 Å were observed, while two-photon lines appeared; and (3) the linewidth, shape, and position of the peaks at 4715 and 4795 Å were unaffected by changing the argon buffer-gas pressure.

The collision cross sections associated with reactions (1a) and (1b) are determined from the relation

$$\sigma = \left[\frac{N(Sr^{+*})}{N(Ca^+)}\right]\left[\frac{1}{N(Sr)\bar{V}\tau}\right], \tag{2}$$

where $N(Sr^{+*})$ is the number density of excited Sr^+ created by the laser-induced charge-transfer process, $N(Ca^+)$ is the number density of ground-state Ca^+ created by the pump laser, $N(Sr)$ is the number density of ground-state Sr neutrals, $\bar{V}$ is the relative speed between Ca ions and Sr neutrals, and τ is the duration of the transfer laser pulse. $N(Sr^{+*})$ is determined from the amplitude of fluorescence as recorded by the photomultiplier and signal processing electronics in conjunction with a calibration of the transmittance of the collection optics. $N(Ca^+)$ is determined by the method of equivalent width[9] from the absorption of a probe laser beam which is scanned through the $Ca^+(4s\ ^2S_{1/2})$-$Ca^+(4p\ ^2P^o_{3/2})$ transition. $N(Sr)$ is also measured by the equivalent width method, with a white-light absorption scan. As an example of the determination of a cross section associated with reaction (1a), the following measurements were made: At a cell temperature of 850 °C, the ground-state Sr density was determined to be $N(Sr)=(2.4\pm1.0)\times10^{16}\ cm^{-3}$. With the pump laser operating at a power density of 4×10^9 W/cm^2, and a ground-state Ca neutral density of $N(Ca)=6\times10^{15}\ cm^{-3}$, the ground-state Ca^+ density was measured to be $N(Ca^+)=(4.5\pm2.4)\times10^{14}$ cm^{-3}. At a transfer laser power density of 1.2×10^8 W/cm^2, the $Sr(5p\ ^2P^o_{3/2})$ density was mea-

sured to be $N(Sr^{+*})=(2.6\pm1.6)\times10^{11}$ cm^{-3}. Thus, with $\bar{V}=9.4\times10^{4}$ cm/s, and $\tau=5\times10^{-9}$ s, Eq. (2) gives $\sigma=(5.1\pm4.6)\times10^{-17}$ cm^2. Further values of collision cross sections for both reactions (1a) and (1b) are plotted as a function of transfer laser power density in Fig. 6.

IV. DISCUSSION

The different experimental results obtained for the different reactions can be explained qualitatively by considering the potential energy curves of the $CaSr^+$ quasimolecule. Figure 7 shows the potential curves which asymptotically approach the initial and final states of reactions (1a) and (1b). These curves result from induced polarizations and van der Waals interactions, and are computed from experimental values of polarizabilites[10] and oscillator strengths.[8,11] It is apparent that the curves associated with the initial and final states of reaction (1a) are very nearly parallel. Hence, the wavelength of the photon which connects these two curves at the R where the maximum transition rate occurs is not detuned very much from the $\lambda_{R=\infty}$ wavelength (4715 Å connects the curves at $R=8.8$ Å; $\lambda_{R=\infty}=4730$ Å). The parallel nature of the curves also results in a narrow linewidth for the laser-induced collision process. In reaction (1b), on the other hand, it is evident from Fig. 7 that the curves associated with the initial and final states of the system are very different from one another. Thus, the photon which connects these curves at the appropriate R is detuned considerably from the $\lambda_{R=\infty}$ photon, and the linewidth is broad (4795 Å connects the curves at $R=8.7$ Å; $\lambda_{R=\infty}=4916$ Å). The reason for the difference in the potential curves of the two reactions is the near coincidence of the $Sr(5p\ ^2P^o_{1/2})$ level with the resonance line of Ca.

The fact that the collision cross section associated with reaction (1a) is larger than that associated with reaction (1b) is a result of two factors. First, the detuning of a photon at 4715 Å relative to the $5s\,5p\ ^1P^o_1$ state of the Sr atom is 500 cm^{-1}, while the detuning of a photon at 4795 Å is 850 cm^{-1}; it is expected that the collision cross section is inversely proportional to the square of this detuning. Second, the nearly parallel quasimolecular potential-energy curves associated with the initial and final states of reaction (1a) imply a long collision interaction time, while the nonparallel curves associated with reaction (1b) imply a short interaction time.

The explanations given above regarding the distinctions between reactions (1a) and (1b) are qualitative in nature. The Landau-Zener formalism[12,13] in conjunction with a widely used form for the charge-transfer interaction Hamiltonian[14] leads to very erroneous predictions for reactions (1a) and (1b), i.e., collision cross sections which are an order of magnitude larger than those measured, and line shapes which peak farther from $\lambda_{R=\infty}$ and are much broader than those observed.

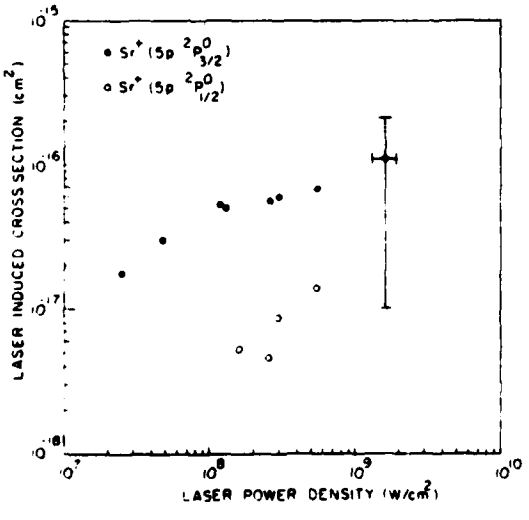

FIG. 6. Laser-induced charge-transfer cross sections as a function of transfer laser power density.

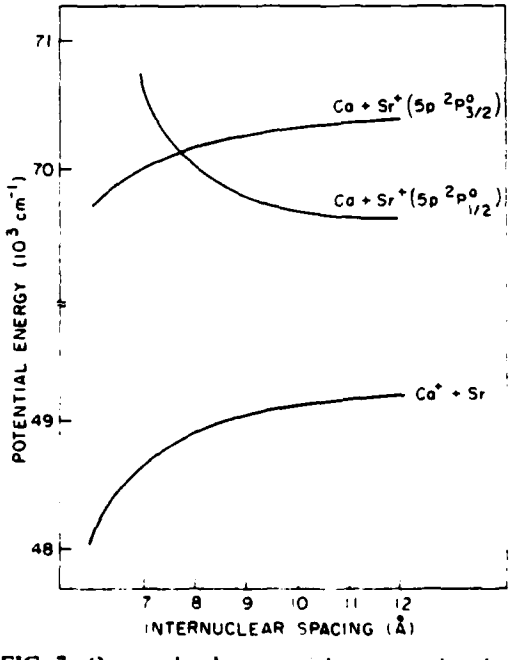

FIG. 7. Quasimolecular potentials associated with reactions (1a) and (1b).

ACKNOWLEDGMENTS

The authors gratefully acknowledge the contributions of B. Yoshizumi and G. Zdasiuk. This work was supported by the U. S. Air Force Office of Scientific Research under Contract No. F49620-80-C-0023.

[1]L. I. Gudzenko and S. I. Yakovlenko, Zh. Tekh. Fiz. 45, 234 (1975) [Sov. Phys.—Tech. Phys. 20, 150 (1975)].

[2]R. Z. Vitlina, A. V. Chaplik, and M. V. Entin, Zh. Eksp. Teor. Fiz. 67, 1667 (1974) [Sov. Phys.—JETP 40, 829 (1974)].

[3]D. A. Copeland and C. L. Tang, J. Chem. Phys. 65, 3161 (1976); 66, 5126 (1977).

[4]M. H. Nayfeh and M. G. Payne, Phys. Rev. A 17, 1695 (1978).

[5]W. R. Green, M. D. Wright, J. F. Young, and S. E. Harris, Phys. Rev. Lett. 43, 120 (1979).

[6]L. S. Goldberg and C. A. Moore, in *Laser Spectroscopy*, edited by R. G. Brewer and A. Mooradian (Plenum, New York, 1974).

[7]N. Dutta, R. Tkach, D. Frohlich, C. L. Tang, H. Mahr, and P. L. Hartman, Phys. Rev. Lett. 42, 175 (1979).

[8]A. Gallagher, Phys. Rev. 157, 24 (1967).

[9]A. P. Thorne, *Spectrophysics* (Chapman and Hall, London, 1974), pp. 307–311.

[10]T. M. Miller and B. Bederson, in *Advances in Atomic and Molecular Physics*, edited by D. R. Bates and B. Bederson (Academic, New York, 1977), Vol. 13, p. 32.

[11]W. L. Wiese, M. W. Smith, and B. M. Miles, *Atomic Transition Probabilities: Volume II, Sodium Through Calcium* (U. S. Government Printing Office, Washington, D. C., 1969), p. 248.

[12]L. D. Landau, Phys. Z. Sowjetunion 2, 46 (1932).

[13]C. Zener, Proc. R. Soc. London A137, 696 (1932).

[14]R. E. Olson, F. T. Smith, and E. Bauer, Appl. Opt. 10, 1848 (1971).